

Article

Remediation of Cd and Cu Contaminated Agricultural Soils near Oilfields by Biochar Combined with Sodium Humate-Wood Vinegar

Junqi Wang¹, Weichun Gao², Junfeng Zhu^{1,3,*} , Yuxiao Yang³ and Yuhua Niu³

¹ The Key Laboratory of Well Stability and Fluid & Rock Mechanics in Oil and Gas Reservoir of Shaanxi Province, Xi'an Shiyou University, Xi'an 710065, China; wjq@xsyu.edu.cn

² Shaanxi Provincial Land Engineering Construction Group, Xi'an 710075, China

³ Shaanxi Key Research Laboratory of Chemical Additives, College of Chemistry and Chemical Engineering, Shaanxi University of Science and Technology, Xi'an 710021, China

* Correspondence: zhujunfeng@sust.edu.cn

Abstract: Soil contaminations by heavy metals near oilfields have been widely reported and are causing great concern. Thus, it is highly desirable to develop cost-effective materials and methods to avoid heavy metal residues contaminating soil and food. An effective, environmentally friendly, and inexpensive remediation material for heavy metal-polluted soil was designed and prepared using biochar (BC) combined with humic acid (HA) resulting from sodium humate (NaHA) simply reacting with wood vinegar (BHW). After adding BHW, the chemical fractions of copper and cadmium in the soil undergo larger changes. Meanwhile, the availability of heavy metals decreases. The maximum adsorption capacity of copper and cadmium in the soil using the BHW is larger than that only using biochar. The adsorption kinetics ensures that the adsorption process of Cd²⁺ and Cu²⁺ ions on BHW is chemical adsorption, which is best fitted using the pseudo-second-order rate equation. The thermodynamics guarantees that the metal ions adsorb on the heterogeneous surface of BHW in multilayer, which is credited to the enhancement of oxygen-containing groups in the biochar combined with the humic acid. The remediation material BHW holds promise for the immobilization of heavy metal in the soils and could be recommended based on its economic feasibility, high efficacy, and environmental safety.

Keywords: heavy metal-contaminated soil; chemical fractions; biochar; humic acid; immobilization mechanism



Citation: Wang, J.; Gao, W.; Zhu, J.; Yang, Y.; Niu, Y. Remediation of Cd and Cu Contaminated Agricultural Soils near Oilfields by Biochar Combined with Sodium Humate-Wood Vinegar. *Agronomy* **2023**, *13*, 1009. <https://doi.org/10.3390/agronomy13041009>

Academic Editors: Hongbiao Cui, Yu Shi, Haiying Lu, Lin Chen and Ru Wang

Received: 26 January 2023

Revised: 11 March 2023

Accepted: 17 March 2023

Published: 29 March 2023



Copyright: © 2023 by the authors. Licensee MDPI, Basel, Switzerland. This article is an open access article distributed under the terms and conditions of the Creative Commons Attribution (CC BY) license (<https://creativecommons.org/licenses/by/4.0/>).

1. Introduction

Heavy metal pollution is a serious global problem, which can cause issues of environmental safety and human health problems. Globally, more than 10 million sites are considered soil contaminated, of which more than 50 percent are polluted with heavy metals [1]. As a cause of rapid economic and societal development, heavy metal soil pollution has increasingly become a serious environmental problem, especially in the field of the petroleum industry and agriculture [2]. The total exceeding standard in China's (China's second-level soil environmental quality standard) soil quality rating is 16.1 percent [3]. The soil of agricultural and industrial areas in China is partially contaminated by heavy metals, and the arable land resources are declining [4]. The blowout accident or leakage in a given oilfield will pollute the surrounding soil and make the heavy metals and other harmful substances seriously invade and damage the soil quality. While applying the waste to the soil, excess heavy metals can cause changes in soil fertility and reduce the size and quality of crop plants [5]. Heavy metals often coexist in contaminated soil and can accumulate in the human body through the food chain of soil crops [6]. Subsequently, heavy metals are absorbed by plants into the food chain and accumulated in animals and humans, where

they can be toxic [7]. In recent years, extensive attention has been paid towards research on environmentally friendly, low-cost materials for soils contaminated by metal [8].

In situ immobilization of heavy metals via chemical stabilization becomes a cost-effective and particularly convenient method to reduce the availability and uptake of heavy metals by plants [9,10]. Biochar (BC) has proved particularly effective in modifying techniques for adsorbing heavy metals and reducing their potential availability [11,12]. The in situ immobilizing of heavy metals in contaminated soil is an effective and low-cost remediation technique to decrease the bioavailability and mobility of toxic elements [6,13]. As a consequence, compared with other remediation technologies such as mechanical separation, chemical washing, and electrodynamic remediation, biochar remediation of contaminated soil has shown special effects on immobilizing heavy metals in soil and reducing the uptake of heavy metals by plants [10,14]. The foremost mechanisms of biochar immobilizing heavy metals in soil include precipitation, increased physical adsorption, enhanced ion exchange capacity, and alkalization [15]. The degree of stable immobilization of heavy metals by biochar is related to the biogeochemical processes that biochar undergoes in soils [16,17]. In particular, the surface properties of biochar are affected by the chemical, physical, and biological processes that are caused by the aging of biochar [18]. Under aerobic conditions, compost produced by spontaneous microbial oxidation of agricultural straw, organic waste and livestock manure has proved to be a very effective soil conditioner for heavy metal contamination [12].

Recently, wood vinegar (WV) has been used to compost solid wastes and charcoal to adsorb and immobilize metal contaminants, such as nickel, zinc, and copper. Wood vinegar can change the structure of organic matter during composting in metal-contaminated soils. The composted organic matter, such as humic acid substances which are important organic matter in soil, can generate insoluble metal-organic compounds, thus lowering the amount of bioavailable metal in the soil [19].

A few previous studies show humic acid or other organic acids can enhance biochar to immobilize and adsorb heavy metals [20,21], such as lead and nickel. At relatively low doses, biochar, humic substances or wood ash can recover pristine soil from multi-contaminated soils and reduce Pb, Cu, and Cd mobility in soils [21]. The formation of complexes between humic acid and Chromium (III) or Chromium (VI) affected the flowability of metal ions and reduced the concentration of free metal species to reduce the heavy metal toxicity of chromium to organisms [22]. Nevertheless, there is very little research on the effects of BC combined with humic acids or other organic acids on the availability and mobility of heavy metals in agricultural soils. The mobility and availability of heavy metals in soils depend on the chemical fractions of them in the soils [12,23]. Therefore, it is necessary to investigate the effect of humic acids or organic acids on biochar interacting with heavy metals, and the subsequent mobility and availability of heavy metals in agricultural soils.

Copper [10] and cadmium [18] are major pollutants in polluting mines, they especially affect farmland near copper mines and oilfields. The mobility and availability of these pollutants are of great concern to China [6,24]. Consequently, this study is focused on agricultural soils contaminated with copper and cadmium [14]. We sought to find out an immobilization material BHW made by BC combined with humic acid resulting from sodium humate simply reacting with wood vinegar. Moreover, wood vinegar is rich in organic acids and generated from the carbonization of wood. The BHW is environmental, high-efficient, economically feasible, and food safe; it therefore holds promise for the recommendation for the remediation of contaminated soils by metals.

2. Materials and Methods

2.1. Soil Samples and Chemicals

The diagram for the experiment route has been presented in Figure S1. A sample of 0–0.20 m surficial soil of agricultural land near the oilfield was taken. The soil was air dried. The soil was purified through a 120-mesh sieve. Then the soil was artificially polluted using a copper nitrate (or cadmium nitrate) solution to prepare a contaminated soil. The chemical

and physical properties of the experimental soil were displayed in Table S1. Based on the 2nd level of heavy metal risk control standard ($400 \text{ mg}\cdot\text{kg}^{-1}$ for copper and $100 \text{ mg}\cdot\text{kg}^{-1}$ for cadmium) of GB15618-2018 of China, the copper nitrate, (or cadmium nitrate) solution including 400 mg Cu^{2+} (or 100 mg Cd^{2+}) was prepared then evenly mixed into 1.0 kg of soil. The contaminated soil samples were cultured for 1 month. The mean value of 3 replicate samples was used for discussion. The information on chemicals in the research was shown in Table S2.

2.2. Preparation Procedure of BHW Remediation Materials

The material composition of every group was expressed in Table S3. We prepared the BHW remediation materials using BC powder, NaHA, and WV solutions having a mass ratio of 1.5:1:1 [25]. BC was mixed with NaHA, crushed thoroughly, dried, and added by WV. The above mixtures were dried in the air to become fine granules. Then the fine granules were sieved by a sifter to get the remediation material. As a control group, under the same experimental conditions, the BC group was composed of only BC used as the control group. In the meantime, under the same processing conditions, the group of BC-NaHA was prepared and consisted of BC and NaHA.

2.3. Remediation Experiment

The six treatment groups for the remediation experiment were respectively named BHW-1, BHW-2, BHW-3, BHW-4, BHW-5, and BHW-6. They were contaminated soils which contain $0.04 \text{ g}\sim 0.5 \text{ g}\cdot\text{kg}^{-1}$ of BHW materials. The same relative quantities of BC-NaHA treatment groups and BC treatment groups were also prepared, respectively. The treatment groups involving BC, BC-NaHA and BHW were shown in Table 1. Each remediation material and the contaminated soil samples were thoroughly blended. Then they were cultured for 30 days under the temperature of $25 \pm 1.0 \text{ }^\circ\text{C}$ and turned several times. After aging, the contaminated soil was employed as a control group without any remediation [25,26]. We prepared 3 replicated samples for every treatment group to guarantee the accuracy of the experimental data.

Table 1. The treatment groups include BC, BC-NaHA and BHW.

	Treatment Dosage ($\text{g}\cdot\text{kg}^{-1}$)	BC	BC-NaHA	BHW
Control group	0	-	-	-
1#	0.04	BC-1	BC-NaHA-1	BHW-1
2#	0.1	BC-2	BC-NaHA-2	BHW-2
3#	0.2	BC-3	BC-NaHA-3	BHW-3
4#	0.3	BC-4	BC-NaHA-4	BHW-4
5#	0.4	BC-5	BC-NaHA-5	BHW-5
6#	0.5	BC-6	BC-NaHA-6	BHW-6

2.4. The Measurement of Metal Content of Different Fractions

The experimental soil samples were cultured in the same environment for 30 days. The metal contents of theirs were detected by the five-point sampling method. Using $0.01 \text{ mol}\cdot\text{L}^{-1}$ CaCl_2 as an extraction agent at the soil-solution ratio of 1:10, the available metal contents in the experimental soil samples were extracted [27,28]. The reduction rate of available copper and cadmium indicates that the incorporation of the remediation material reduces the percentage content of available copper and cadmium compared to the control sample [21,27]. It was necessary to quantify the available, exchangeable and reducible fractions after the remediation treatment for assessing metal mobility [29]. According to Table S4, the chemical compositions of Cu and Cd in control soil and BHW-restored soil were performed using the BCR (European Community Bureau of Reference) sequential extraction method [30].

The contents of Cu^{2+} and Cd^{2+} ions in different fractions were determined by a graphite furnace atomic absorption spectrometer (AAS) [26]. The sample solution was prepared to 100 mL with deionized water and then filtered with a 0.22 μm filter. After that, the filtrate solution was used to measure the content of soluble Cu^{2+} and Cd^{2+} ions by the AAS. The detailed parameters of measurement were followed. The photomultiplier tube voltage is 540 V, at the same time, the lamp current is 7.5 mA. Besides, the slit was 1.3 nm, and the wavelength was 283.3 nm. The atomization temperature was 1900 °C and the ashing temperature was 650 °C [26]. Three replicates were carried out for every sample and the mean value of 3 replicates was used for the research.

2.5. Adsorption Properties of Remediation Materials

2.5.1. Adsorption Kinetics

Using 0.01 $\text{mol}\cdot\text{L}^{-1}$ of NaNO_3 as background, Cu^{2+} solution and Cd^{2+} solution were prepared in two 1000 mL beakers, their initial concentrations were 400 $\text{mg}\cdot\text{L}^{-1}$ and 100 $\text{mg}\cdot\text{L}^{-1}$, respectively. Under the temperature of 25 ± 0.5 °C, stirring with a thermostatic magnetic stirrer, 0.5 g of BHW was added into the solution with Cu^{2+} or the Cd^{2+} solution. At the adsorption time of 5, 10, 30, 60, 120, 180, 240, 360, 480, 600, 720, and 1440 min, the solution samples were quickly drawn with a pipette to pass through a 0.22 μm filter membrane. The content of copper and cadmium in the filtrate was measured to measure their adsorption capacity by an AAS, respectively.

2.5.2. Adsorption Isotherms

0.2 g BHW was put in a 50 mL polyethylene centrifuge tube, after that, with 0.01 $\text{mol}\cdot\text{L}^{-1}$ NaNO_3 as the background, a 20 mL Cu^{2+} solution was added to the 50 mL polyethylene centrifuge tube. Then, the original concentrations of the cadmium solutions were set as 5, 10, 20, 50, 80, 100, 200, and 300 $\text{mg}\cdot\text{L}^{-1}$. Meantime, the original concentrations of the copper solutions were set as 10, 20, 50, 80, 100, 200, 300, 400, 500, and 600 $\text{mg}\cdot\text{L}^{-1}$. The volume of all solutions was set as 50 mL. Then the centrifuge tube was oscillated at 200 $\text{r}\cdot\text{min}^{-1}$ for 24 h in a shaking incubator with a constant temperature of 15 °C, 25 °C and 35 °C, respectively. After oscillation, the sample was centrifuged using a centrifuge at 8×10^3 $\text{r}\cdot\text{min}^{-1}$ for 10 min. In succession, the supernatant solution was filtered by a 0.22 μm filter membrane. Then the concentration of copper and cadmium in the filtrate was measured by the AAS, and the adsorption capacity of BHW was calculated.

2.5.3. Competitive Adsorption

The partition coefficient was an important parameter describing the adsorption characteristics of heavy metals in the soil. This was particularly crucial to determine the selection order of remediation materials under the co-competitive action of multiple metal ions through the distribution coefficient. A 0.5 g of soil without BHW was set as Soil-A. A 0.5 g of soil containing 0.2% BHW was set as Soil-B. They were put into 100 mL polyethylene centrifuge tubes, respectively. Two groups of 50 mL mixed solutions contained three initial concentrations of 100, 200 and 300 $\text{mg}\cdot\text{L}^{-1}$ of Cd^{2+} and Cu^{2+} , respectively. The pH value of the solutions was 5.0. The two groups of blended solutions were poured into Soil-A and Soil-B, respectively. The blended solutions were centrifuged at 8×10^3 $\text{r}\cdot\text{min}^{-1}$ for 10 min, and after oscillated at a constant temperature (25 ± 0.5 °C) for 24 h. The supernatant solutions were passed through a 0.22 μm filter. The concentrations of heavy metals in the filtrate were measured and the adsorption capacity was calculated.

$$K_d = \frac{Q_e}{C_e} \quad (1)$$

where, K_d is the distribution coefficient of heavy metals at the soil-water interface; C_e means the equilibrium concentration of metal ions in the blended solution, $\text{mg}\cdot\text{g}^{-1}$; Q_e refers to the capacity of metals adsorbed by the soil, $\text{mg}\cdot\text{g}^{-1}$.

2.6. Data Statistics

2.6.1. Adsorption Capacity

The amount of adsorption of heavy metals was calculated according to the following formula:

$$Q_e = \frac{C_0 - C_e}{m} \times \frac{V}{1000} \quad (2)$$

where, Q_e refers to the amount of adsorption of metals, $\text{mg}\cdot\text{g}^{-1}$; C_0 means the initial concentration of metals, $\text{mg}\cdot\text{L}^{-1}$; V represents the volume of the solution, mL; m is the mass of the soil sample, g; C_e means the equilibrium concentration of metals, $\text{mg}\cdot\text{L}^{-1}$.

2.6.2. Adsorption Kinetic

(1) Pseudo first-order rate equation

$$\ln(Q_e - Q_t) = \ln Q_e - K_1 t \quad (3)$$

where, Q_e refers to the adsorption amount at equilibrium, $\text{mg}\cdot\text{g}^{-1}$; Q_t means the adsorption amount at the time t , $\text{mg}\cdot\text{g}^{-1}$; K_1 is the pseudo-first-order rate constant, min^{-1} ; t represents the reaction time, min.

(2) Pseudo-second-order rate equation

$$\frac{t}{Q_t} = \frac{t}{Q_e} + \frac{1}{K_2 Q_e^2} \quad (4)$$

where, Q_e refers to the adsorption amount at equilibrium, $\text{mg}\cdot\text{g}^{-1}$; Q_t means the adsorption amount at the time of t , $\text{mg}\cdot\text{g}^{-1}$; K_2 is the pseudo-second-order rate constant, min^{-1} ; t represents the reaction time, min.

2.6.3. Adsorption Isotherm

(1) Langmuir adsorption isotherm

$$\frac{C_e}{Q_e} = \frac{C_e}{Q_{max}} + \frac{1}{K_L Q_{max}} \quad (5)$$

where, C_e refers to the concentration at adsorption equilibrium, $\text{mg}\cdot\text{L}^{-1}$; Q_e represents the adsorption capacity at equilibrium, $\text{mg}\cdot\text{g}^{-1}$; K_L means a constant related to the size of the adsorption energy, $\text{L}\cdot\text{mg}^{-1}$; Q_{max} refers to the adsorption capacity at maximum, $\text{mg}\cdot\text{g}^{-1}$.

(2) Freundlich adsorption isotherm

$$\ln Q_e = \frac{1}{n} \ln C_e + \ln K_F \quad (6)$$

where, C_e refers to the concentration at adsorption equilibrium, $\text{mg}\cdot\text{L}^{-1}$; K_F represents a constant related to the adsorption strength, $\text{mg}\cdot\text{g}^{-1}$; Q_e means the adsorption amount at equilibrium, $\text{mg}\cdot\text{g}^{-1}$; n refers to the heterogeneity of the adsorbent. The factor, when $n > 1$, indicates that there is a strong force between the adsorbate and the adsorbent.

All data of this work are analyzed by the single-factor analysis of variance, the data is the mean \pm standard deviation, and lowercase letters indicate significant differences between different groups under the same percentage ($p < 0.05$).

2.7. Fourier Transform Infrared Spectroscopy and X-ray Photoelectron Spectrometer Measurements

All BHW, BC-NaHA, BC and their immobilization samples were rinsed three times with ultrapure water before and after immobilizing metal ions to remove all the physisorbed metal ions. Then under vacuum, the samples were dried overnight for all measure-

ments [17,25]. Using the KBr disc technique, Fourier Transform Infrared Spectroscopy (FT-IR) spectra of the samples were carried out by a VECTOR-22 Fourier transform infrared spectrometer (Bruker, Germany) [23].

X-ray Photoelectron Spectrometer (XPS) test was run by an XPS spectrometer (AXIS Supra type, Kratos, UK). The spectra of all BHW, BC-NaHA, BC and their immobilization samples were obtained over the range of 0 to 1200 eV. The slit width of the analyzer was 1.9 mm and in energy the analyzer was 300 eV. The binding energy was calibrated using the C1s peak as 284.60 eV [25,31,32].

3. Results and Discussion

3.1. Effect of BHW on the Availability of Cu and Cd

Figure 1 displays the effects of different dosages and types of restoration materials on the available copper and cadmium content in the soil. The addition of BHW material significantly reduced the effective Cu^{2+} and Cd^{2+} content extracted by CaCl_2 , and the effective Cu^{2+} and Cd^{2+} content of the three materials was the lowest. Compared with the control group (Figure 1a), at the addition level of $0.8 \text{ g}\cdot\text{kg}^{-1}$, BC, BC-NaHA, and BHW reduced the effective content of copper by 28.88%, 38.76%, and 47.50%, respectively, which is higher than the report of Rong et al. [33] that humic acid reduces the effective Cu^{2+} content by 18%. Compared with the control group (Figure 1b), when the added amount was $1.6 \text{ g}\cdot\text{kg}^{-1}$, BC, BC-NaHA, and BHW reduced the effective content of copper by 16.67%, 30.14%, and 38.47%, respectively. This is higher than the result of Rong et al. [33] that humic acid reduces the effective Cd^{2+} content by 37%. This implies that the addition of wood vinegar can enhance the ability of BC-NaHA to adsorb copper and cadmium ions. In other words, BHW has a better solidification effect on Cu^{2+} and Cd^{2+} ions in the soil at a lower dose and has a significant effect on reducing the available content of copper and cadmium.

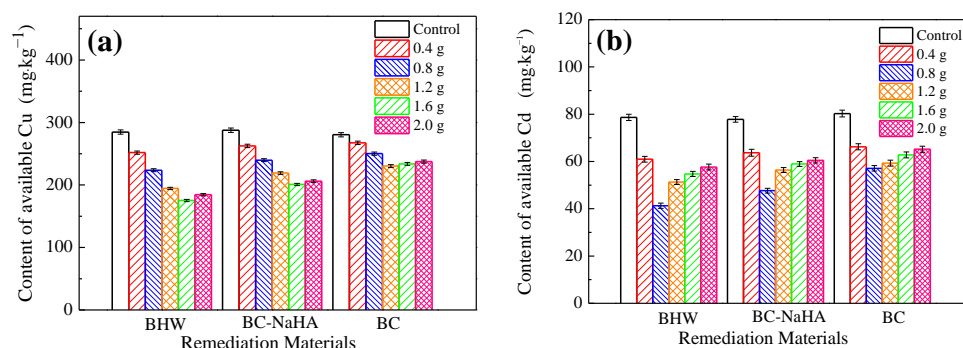


Figure 1. The effect of different restoration materials on the available copper (a) and cadmium (b) in the soil.

3.2. Effect of BHW on the Chemical Fractions of Cu and Cd

Figure 2 shows the changes in the chemical forms of copper and cadmium in the soil before and after BHW material treatment. After treatment with 0.8 g of BHW material (Figure 2a), the exchangeable and reducible components of Cu^{2+} decreased by 9.30% and 11.79%, respectively. At the same time, the Cu^{2+} of the oxidizable component and the residue component rise by 5.47% and 15.62%, respectively, and the results of the copper form transformation law are consistent with the literature [34,35]. After treatment with 1.6 g of BHW material (Figure 2b), the exchangeable and reducible components of Cd^{2+} decreased by 12.08% and 4.80%, respectively. At the same time, the Cd^{2+} of the oxidizable component and the residual component rise by 8.28% and 15.58%, respectively. The results of the cadmium form transformation law are consistent with the literature [34,35]. Therefore, BHW can effectively reduce the Cu^{2+} and Cd^{2+} contents of the exchangeable and reduced components in the soil, thereby reducing the toxicity and bioavailability of copper and cadmium [19].

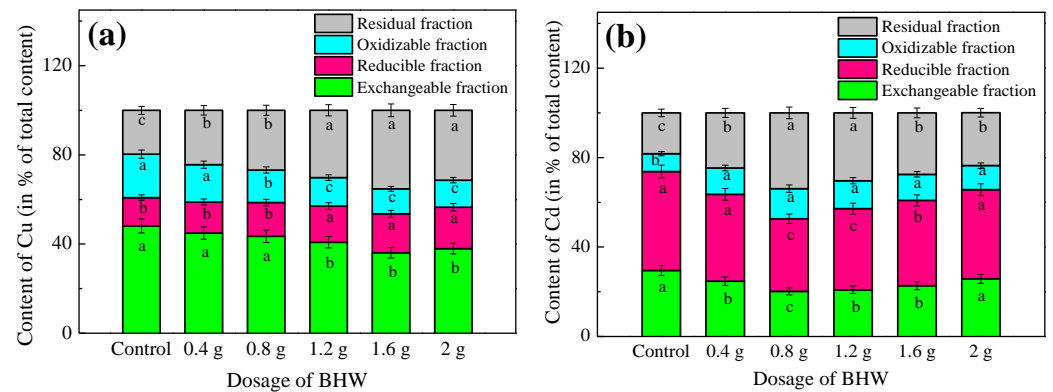


Figure 2. The effect of the amount of BHW material on the chemical fractions of copper (a) and cadmium (b) in the soil. Bars mean standard deviation and the data refer to means \pm standard deviation ($n = 3$). Lowercase letters represent significant differences at $p < 0.05$ between different treatments at the same fraction.

3.3. Effect of BHW on Competitive Adsorption

Under the condition of the coexistence of binary heavy metals, the competitive adsorption of binary heavy metals on soil (Soil-A) is shown in Figure 3a, and the competitive adsorption of binary heavy metals on BHW-containing soil (Soil-B). As shown in Figure 3b. At the initial concentration which is set in the experiment, the adsorption amount Q_e of binary heavy metals on Soil-A and Soil-B is in the order of $\text{Cu}^{2+} > \text{Cd}^{2+}$.

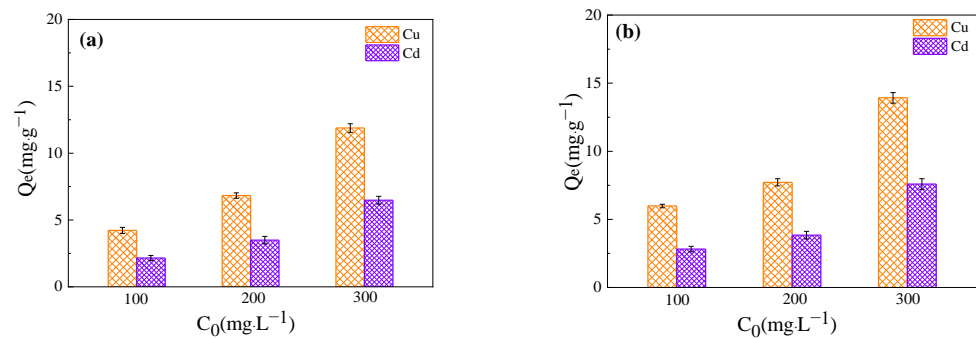


Figure 3. (a) Competitive adsorption diagram of dual heavy metals in Soil-A; (b) Competitive adsorption diagram of dual heavy metals in Soil-B.

Table 2 shows the partition coefficient and joint partition coefficient $K_{d\Sigma\text{sp}1}$ of each metal in soil without BHW (Soil-A), and the partition coefficient and joint partition coefficient $K_{d\Sigma\text{sp}2}$ of each metal in soil with BHW (Soil-B). In soil and BHW-containing soil systems, the order of the partition coefficient of the Cu-Cd competition system is $\text{Cu} > \text{Cd}$, and the priority order of adsorption is $\text{Cu} > \text{Cd}$, which is in line with the results reported in the literature [9]. The joint partition coefficient $K_{d\Sigma\text{sp}2}$ of soil heavy metals with BHW is higher than the joint partition coefficient $K_{d\Sigma\text{sp}1}$ of soil without BHW, which indicates that BHW increases the rate of soil rapid adsorption of Cu^{2+} and Cd^{2+} ions.

Table 2. The partition coefficient and joint partition coefficient at different initial concentrations of metal ions.

Partition Coefficient	Soil-A		$K_{d\Sigma sp1}$	Soil-B		$K_{d\Sigma sp2}$
	Cu	Cd		Cu	Cd	
K_{d100}	0.073	0.028	0.101	0.149	0.039	0.188
K_{d200}	0.052	0.021	0.073	0.063	0.024	0.087
K_{d300}	0.066	0.028	0.094	0.087	0.034	0.121

3.4. Adsorption Kinetic

Figure 4a presents the change in the capacity of Cu^{2+} and Cd^{2+} ions adsorbed by BHW over time. From Figure 4a, the adsorption amount of BHW for Cu^{2+} ions rose rapidly in the first 60 min, slowly increased in 60–120 min, and gradually reached equilibrium at 180 min, the equilibrium adsorption capacity was $43.60 \text{ mg}\cdot\text{g}^{-1}$. The adsorption capacity of Cd^{2+} ions by BHW increased rapidly in the first 120 min, the slow ascending stage was 120–180 min, and gradually reached equilibrium at 240 min, and the equilibrium adsorption capacity was $26.66 \text{ mg}\cdot\text{g}^{-1}$. The reason is that there are abundant adsorption sites on the BHW surface at the initial stage of adsorption. After Cu^{2+} and Cd^{2+} ions occupied the sites rapidly, the surface-active vacancy sites of BHW were greatly reduced. Cu^{2+} and Cd^{2+} ions began to penetrate BHW, resulting in a decreased adsorption rate. As the adsorption time increases, the amount of Cu^{2+} and Cd^{2+} ions absorbed by BHW also increases, because the concentration difference driving force of the solution at high concentration promotes the infiltration of Cd^{2+} and Cu^{2+} ions into BHW material, and the utilization rate of adsorption sites expands.

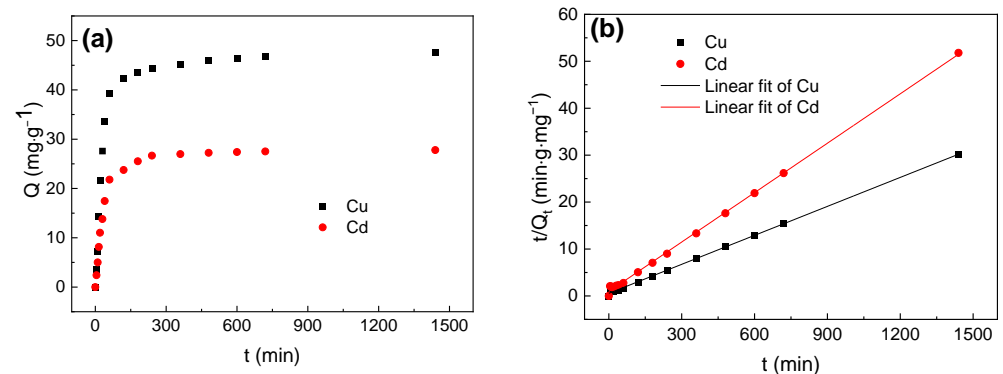
**Figure 4.** (a) BHW adsorption of Cd^{2+} and Cu^{2+} ions change curve with adsorption time; (b) Linear fitting diagram of pseudo-second-order rate equation.

Figure 4b shows the linear fitting curve diagram of the pseudo-second-order rate equation. The adsorption rate of Cu^{2+} ions by BHW is much faster than that of Cd^{2+} ions. Table 3 shows the corresponding fitting parameters and calculation parameters of the pseudo-first-order and pseudo-second-order rate equations for the adsorption of Cd^{2+} and Cu^{2+} ions by BHW. In comparison, the calculated values of the pseudo-second-order rate equation ($Q_{e,cal} = 48.54 \text{ mg}\cdot\text{g}^{-1}$ and $28.49 \text{ mg}\cdot\text{g}^{-1}$) are the closest to the experimental values of equilibrium adsorption capacity ($Q_{e,exp} = 43.60 \text{ mg}\cdot\text{g}^{-1}$ and $26.66 \text{ mg}\cdot\text{g}^{-1}$). This indicates that this kinetic equation is more suitable to describe the adsorption process of Cu^{2+} and Cd^{2+} ions on BHW. The fitting parameters (R^2) of the pseudo-second-order rate equation ($R^2 = 0.9989$) are higher, indicating that chemical sorption is the main adsorption of Cu^{2+} and Cd^{2+} ions by BHW material [6].

Table 3. Fitting parameters of adsorption kinetics of BHW adsorption of Cd²⁺ and Cu²⁺.

Linear Model Type	Parameters	Cu ²⁺	Cd ²⁺
Quasi-first-order	Q_e (mg·g ⁻¹)	42.53	22.57
	K_1 (min ⁻¹)	0.0316	0.0175
	R^2	0.9766	0.9609
Quasi-second-order	Q_e (mg·g ⁻¹)	48.54	28.49
	K_2 (g·mg ⁻¹ ·min ⁻¹)	0.000757	0.001293
	R^2	0.9985	0.9989

3.5. Adsorption Isotherms

Figure 5a indicates the relationship between the adsorption capacity of Cd²⁺ and Cu²⁺ ions on BHW and the initial concentration of BHW, respectively. At the same initial concentration, the adsorption capacity of Cd²⁺ and Cu²⁺ ions on BHW gradually increases as the temperature increases. It indicates that the interaction between the adsorbent and solvent surface is reduced with increasing temperature, and more adsorption sites are released, which promoted the adsorption of metal ions.

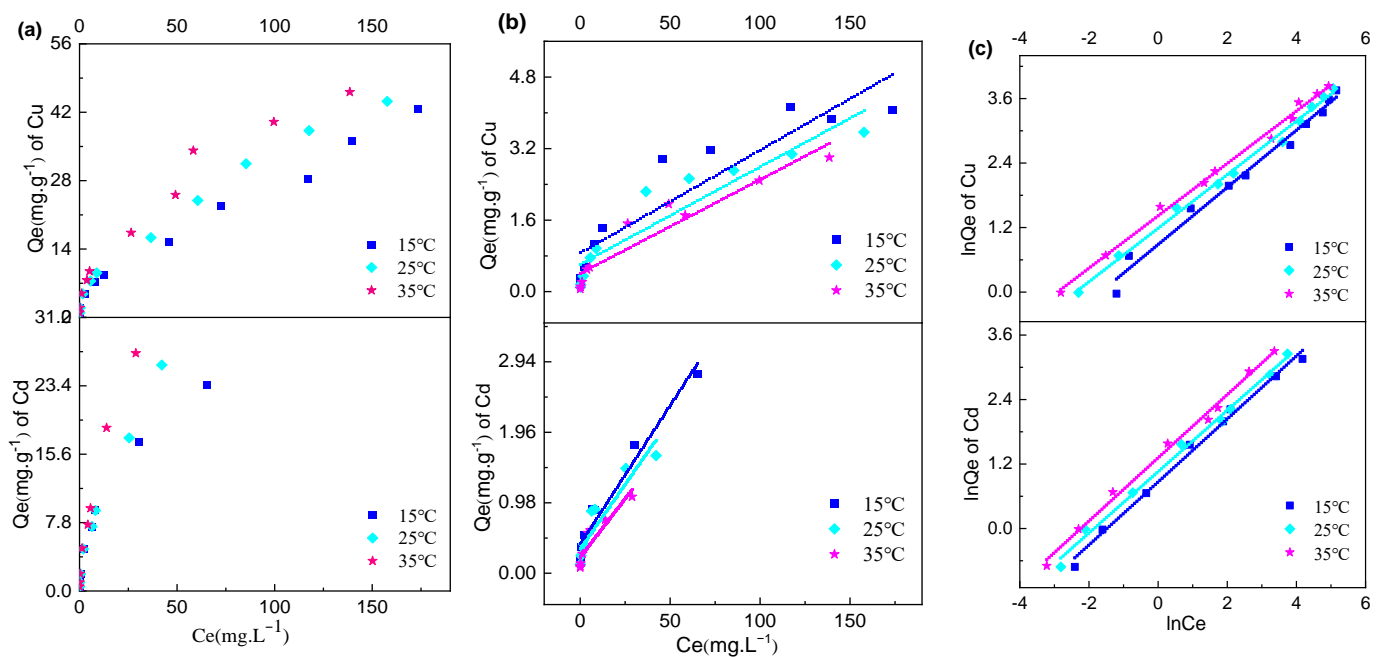
**Figure 5.** (a) The influence of initial concentration on the adsorption capacity of Cd²⁺ and Cu²⁺ ions of BHW; (b) the linear fitting of the *Langmuir* model; (c) the linear fitting of the *Freundlich* model.

Figure 5b,c are respectively the linear fitting diagrams of the *Freundlich* model and *Langmuir* model for Cd²⁺ and Cu²⁺ adsorption isotherms in the presence of BHW. The related parameters are expressed in Table 4. The *Freundlich* model has a better fit to the experimental results of Cd²⁺ and Cu²⁺ ions, it predicts that Cd²⁺ and Cu²⁺ ions form multilayer adsorption on the surface of the adsorbent BHW while being accompanied by chemical reactions. The maximum adsorption amount of BHW on Cd²⁺ and Cu²⁺ ions is higher than that of the humic acid-based carbon material in the literature [21]. The values of n are greater than 1 and between 1–10, which indicates that Cu²⁺ and Cd²⁺ ions are easy to adsorb on BHW [36]. When the temperature is 288.15 K, 298.15 K, and 308.15 K, the K_F value of the *Freundlich* model rises with the increase in temperature. The temperature rise is beneficial to reduce the interaction between the adsorbent and the solvent surface because the larger the value of K_F , the more the adsorption amount. Consequently, more adsorption sites are exposed, which promotes the adsorption of metal ions on the BHW material. The fitting parameter K_F of Cu²⁺ adsorption on the BHW material is greater than that of Cd²⁺,

which proves that the adsorption of Cu^{2+} ions by BHW is faster than the adsorption of Cd^{2+} ions at the same temperature. It is consistent with the result of the dynamics section.

Table 4. Fitting parameters of adsorption thermodynamics for BHW adsorption of Cd^{2+} and Cu^{2+} .

Fitting Type	Parameters	Cu(II)			Cd(II)		
		288.15 K	289.15 K	308.15 K	288.15 K	289.15 K	308.15 K
Langmuir	Q_{\max} ($\text{mg}\cdot\text{g}^{-1}$)	43.48	45.87	47.62	25.91	27.86	30.67
	K_L ($\text{L}\cdot\text{mg}^{-1}$)	0.0266	0.0356	0.0514	0.0954	0.1065	0.1457
	R^2	0.8526	0.8751	0.9071	0.9566	0.8569	0.8457
Freundlich	K_F ($\text{mg}\cdot\text{g}^{-1}$)	2.418	3.276	4.128	2.376	2.875	3.721
	n	1.88	2.006	2.052	1.706	1.752	1.701
	R^2	0.9844	0.9945	0.9949	0.9926	0.9937	0.9946

3.6. Immobilization Mechanism

FT-IR spectra of BC, BC-NaHA, and BHW are shown in Figure 6a. The intensities of the -OH, C=C, C=O, and C-O peaks of the BHW material are much greater than those of the corresponding peaks on the BC, and BC-NaHA materials [37–39]. The order of the number of functional groups is BHW > BC-NaHA > BC. The results show that the introduction of WV can enhance the quantity of oxygen-containing groups, increase the adsorption sites on the surface of the material, and can adsorb more metal ions to form metal complexes. Figure 6b shows the FT-IR spectra of Cu^{2+} ions immobilized by BC, BC-NaHA, and BHW. The intensity of hydroxyl peaks on the three materials decreases significantly after Cu^{2+} ion adsorption, among which the absorption peaks of carboxyl and hydroxyl groups weaken significantly after Cu^{2+} ion adsorption by BHW [40,41]. It indicates that compared with BC-NaHA and BC, both hydroxyl and carboxyl groups on BHW materials are involved in the reaction with Cu^{2+} ion. This is consistent with the research results of the literature [42]. Figure 6c shows the FT-IR spectra of Cd^{2+} ions before and after adsorption by BC, BC-NaHA and BHW. After Cd^{2+} ions were immobilized by BC, BC-NaHA, and BHW, the stretching vibration peaks of hydroxyl (-OH), aromatic C=C, C=O, and C-O were reduced, respectively, and the hydroxyl and carboxyl groups on BHW had the most significant weakening effect. It indicates that a large number of hydroxyl and carboxyl groups on BHW react with Cd^{2+} ions to form more metal complexes, which is in line with the research results of Bai et al. [41].

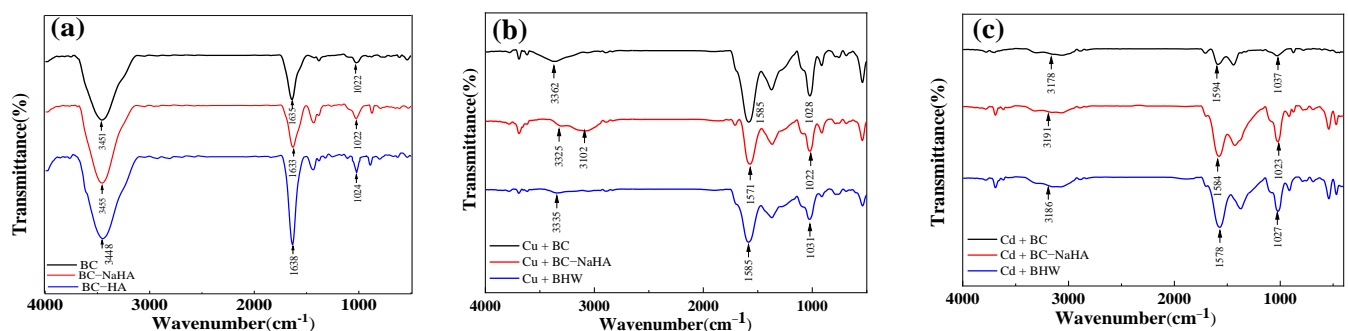


Figure 6. (a) FT-IR spectra of Cu^{2+} ions immobilized by BC, BC–NaHA, and BHW; (b) FT-IR spectra of Cu^{2+} ions immobilized by BC, BC–NaHA, and BHW; (c) FT-IR spectra of Cd^{2+} ions immobilized by BC, BC–NaHA, and BHW.

XPS full spectrum of BC, BC-NaHA, and BHW before and after Cd^{2+} and Cu^{2+} ion adsorption is shown in Figure 7. It can be seen from Figure 7, that there are peaks of Na1S and Ca2P on BHW and BC-NaHA materials, but the peaks of Na1S and Ca2P disappear after Cd^{2+} and Cu^{2+} ions are absorbed. The main reason is that Cd^{2+} and Cu^{2+} ions

are complexed with BC-NaHA and BHW oxygen-containing functional groups by ion-exchange, instead of Na(i) ions and Ca²⁺ ions [12].

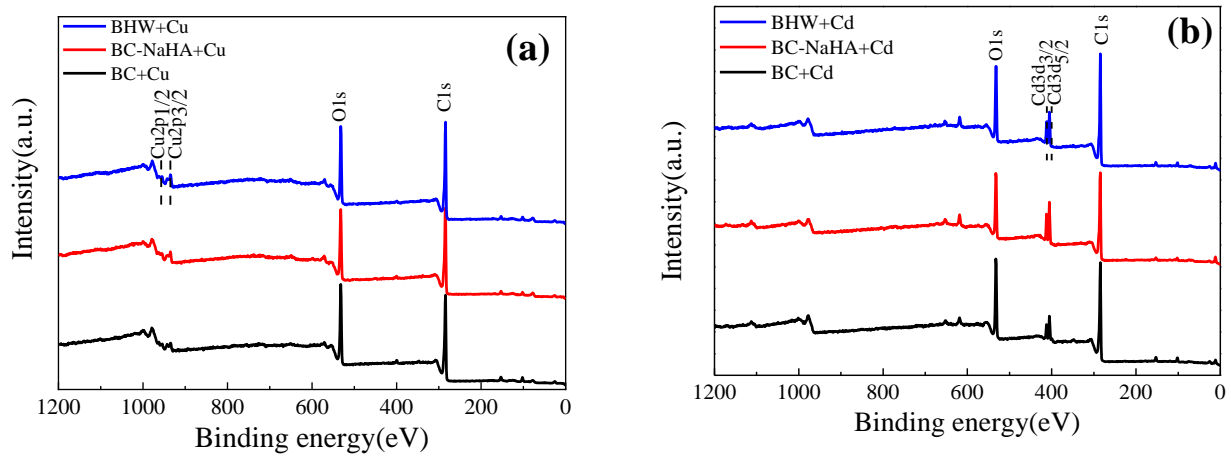


Figure 7. (a) XPS full spectrum of BC, BC-NaHA, and BHW before and after Cu²⁺ ion adsorption; (b) XPS full spectrum of BC, BC-NaHA, and BHW before and after Cd²⁺ ion adsorption.

Figure 8 indicates the C1s high-resolution spectra before and after the adsorption of Cu²⁺ (or Cd(II)) ions by BC, BC-NaHA and BHW. As shown in Figure 8a, C=C/C-C, O-C=O and C-OH in the C1s spectrum are located at 284.60 eV, 288.65 eV and 286.10 eV, respectively [22,32]. Before immobilizing heavy metal ions, the contents of C=C/C-C, O-C=O and C-OH in the spectrum of BC are 66.4%, 13.2% and 20.4%, respectively. As for BC-NaHA, the content of C=C/C-C, O-C=O and C-OH in the spectrum are 59.90%, 12.7% and 27.4%, respectively. However, the contents in the BHW spectrum are 51.1%, 11.1% and 37.8%, respectively. The result shows that the BHW material has the highest oxygen content (48.9%) among the three materials, followed by BC-NaHA (40.1%) and BC (33.6%) due to the introduction of more oxygen-containing functional groups by wood vinegar.

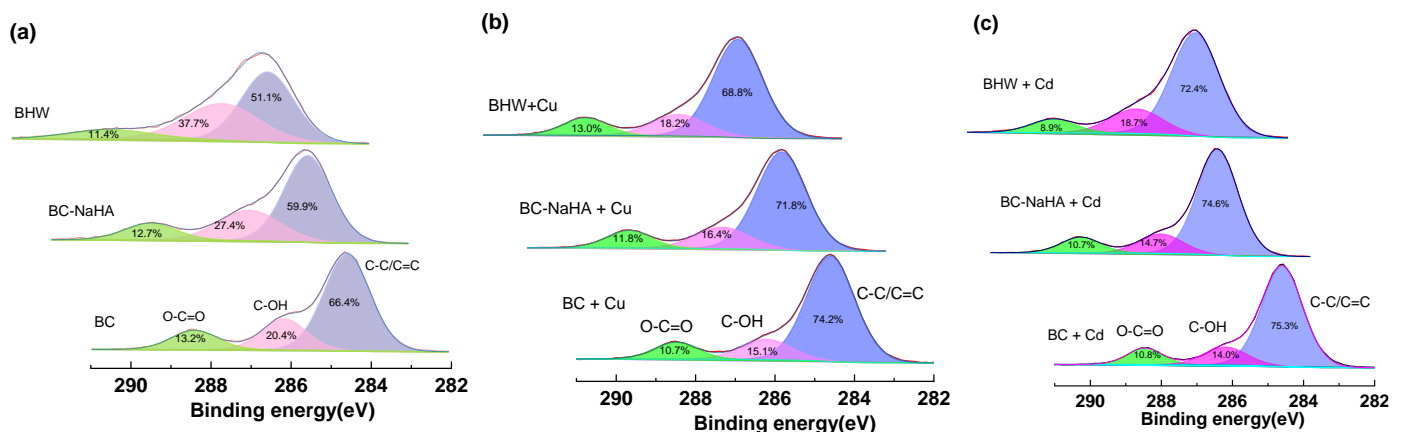


Figure 8. C1s high-resolution spectra of BC-NaHA and BHW before (a) and after adsorbing Cu²⁺ ion (b) and Cd²⁺ ion (c).

After immobilizing Cu²⁺ (or Cd(II)) ions in Figure 8b,c, the contents of C=C/C-C, O-C=O and C-OH in the BC spectrum are 74.2% (75.3%), 10.74% (10.8%), and 15.10% (14.0%), respectively. The contents are 71.8% (74.6%), 11.8% (10.6%), and 16.4% (14.7%) in the BC-NaHA spectrum, respectively. However, they are 68.8% (72.4%), 13.0% (8.9%), and 18.2% (18.7%), respectively. The result shows that the oxygen contents decrease by 7.8% (8.9%), 17.9% (21.5%), and 11.9% (14.7%), respectively. Compared with the oxygen contents before immobilization, all the oxygen contents significantly reduce, and the oxygen

contents of BHW dramatically decrease. Therefore, the hydroxyl and carboxyl groups of BHW and metal ions formed more metal complexes. This result is consistent with that of FT-IR analysis [43].

4. Conclusions

Biochar combined with sodium humate-wood vinegar enhances the ability of soil to absorb and solidify heavy metal ions and reduces the bioavailability of heavy metals; the priority order of adsorption for multiple metals is $\text{Cu} > \text{Cd}$. Applying 0.01–0.16% of BHW material, the exchangeable and reducible content is significantly reduced, and the content of oxidizable components and residues is significantly increased; the reduction rate of effective content reaches 38.47–61.40%. The adsorption curve of BHW adsorption of Cd^{2+} and Cu^{2+} shows the *Freundlich* model for multilayer adsorption. It has better adsorption performance when the pH value is 5–6. BHW materials have obvious chemical adsorption characteristics for pollutants. The heterogeneous structure increases the pore structure, increases the adsorption surface area, and has more active sites. The adsorption mechanisms include chemical adsorption, surface physical adsorption, ion exchange, electrostatic interaction, and coordination. This work provides scientific guidance for the development of low-cost, widely applicable soil remediation materials and application techniques, which can be used on soil contaminated by heavy metals.

Supplementary Materials: The following supporting information can be downloaded at: <https://www.mdpi.com/article/10.3390/agronomy13041009/s1>, Figure S1. The diagram for the experiment route; Table S1. The chemical and physical properties of experimental soil; Table S2. The information on chemicals in the research; Table S3. The material composition of each group; Table S4. BCR sequential extraction process for Cu and Cd of soil samples.

Author Contributions: Supervision, project administration, J.W.; conceptualization, methodology, writing—review and editing, J.Z.; investigation, formal analysis, writing—original draft preparation, W.G.; visualization, Y.Y.; resources, Y.N. All authors have read and agreed to the published version of the manuscript.

Funding: This work was funded by the Key Laboratory of Well Stability and Fluid & Rock Mechanics in Oil and Gas Reservoir of Shaanxi Province, Xi'an Shiyou University (grant number: WSRM20200303001), the Shaanxi Province Key R&D Program (Grant number: 2021SF-431), the Key Research & Development Plan Project of Shaanxi Province of China (Grant number: 2023-YBSF-313), the Key Laboratory of Degraded and Unused Land Consolidation Engineering, the Ministry of Natural Resources of the People's Republic of China (Grant number: SXDJ2018-01), and Shaanxi Province Rural Vitalization Science and Technology Project (Grant number: 2022FP-10).

Data Availability Statement: The datasets used and/or analysed during the current study are available from the corresponding author upon reasonable request.

Acknowledgments: We acknowledge Guodong Fan provides help on XPS analysis. We also acknowledge Bo Wang and Chengkun Liu for their help on resources.

Conflicts of Interest: The authors declare no conflict of interest.

References

1. Lwin, C.S.; Seo, B.H.; Kim, H.U.; Owens, G.; Kim, K.R. Application of soil amendments to contaminated soils for heavy metal immobilization and improved soil quality—A critical review. *Soil Sci. Plant Nutr.* **2018**, *64*, 156–167. [CrossRef]
2. Yang, Q.; Li, Z.; Lu, X.; Duan, Q.; Huang, L.; Bi, J. A review of soil heavy metal pollution from industrial and agricultural regions in China: Pollution and risk assessment. *Sci. Total Environ.* **2018**, *642*, 690–700. [CrossRef] [PubMed]
3. MEP of China (Ministry of Environmental Protection of China). Soil Pollution Control Action Plan. 2016. Available online: https://zsmepgovcn/fg/gwyw/201605/t20160531_352665.shtml (accessed on 1 January 2021).
4. Fei, X.; Christakos, G.; Xiao, R.; Ren, Z.; Liu, Y.; Lv, X. Improved heavy metal mapping and pollution source apportionment in Shanghai city soils using auxiliary information. *Sci. Total Environ.* **2019**, *661*, 168–177. [CrossRef] [PubMed]
5. Szatyłowicz, E.; Krasowska, M. Assessment of heavy metals leaching from fly ashes as an indicator of their agricultural use. *Desalin. Water Treat.* **2020**, *199*, 288–296. [CrossRef]

6. Li, H.; Ye, X.; Geng, Z.; Zhou, H.; Guo, X.; Zhang, Y.; Zhao, H.; Wang, G. The influence of biochar type on long-term stabilization for Cd and Cu in contaminated paddy soils. *J. Hazard. Mater.* **2016**, *304*, 40–48. [[CrossRef](#)] [[PubMed](#)]
7. Palansooriya, K.N.; Shaheen, S.M.; Chen, S.S.; Tsang Daniel, C.W.; Hashimoto, Y.; Hou, D.; Bolan, N.S.; Rinklebe, J.; Ok, Y.S. Soil amendments for immobilization of potentially toxic elements in contaminated soils: A critical review. *Environ. Int.* **2020**, *134*, 105046. [[CrossRef](#)]
8. Yang, T.; Hodson, M.E. Investigating the use of synthetic humic-like acid as a soil washing treatment for metal contaminated soil. *Sci. Total Environ.* **2019**, *647*, 290–300. [[CrossRef](#)]
9. Abbas, T.; Rizwan, M.; Ali, S.; Zia-ur-Rehman, M.; Qayyum, M.F.; Abbas, F.; Hannana, F.; Rinklebe, J.; Ok, Y.S. Effect of biochar on cadmium bioavailability and uptake in wheat (*Triticum aestivum* L.) grown in a soil with aged contamination. *Ecotoxicol. Environ. Saf.* **2017**, *140*, 37–47. [[CrossRef](#)]
10. Brennan, A.; Jiménez, E.M.; Puschenreiter, M.; Albuquerque, J.A.; Switzer, C. Effects of biochar amendment on root traits and contaminant availability of maize plants in a copper and arsenic impacted soil. *Plant Soil* **2014**, *379*, 351–360. [[CrossRef](#)]
11. Cha, J.S.; Park, S.H.; Jung, S.C.; Ryu, C.; Jeon, J.K.; Shin, M.C.; Park, Y.K. Production and Utilization of Biochar: A Review. *J. Ind. Eng. Chem.* **2016**, *40*, 1–15. [[CrossRef](#)]
12. Liang, J.; Yang, Z.; Tang, L.; Zeng, G.; Yu, M.; Li, X.; Wu, H.; Qian, Y.; Li, X.; Luo, Y. Changes in heavy metal mobility and availability from contaminated wetland soil remediated with combined biochar-compost. *Chemosphere* **2017**, *181*, 281–288. [[CrossRef](#)] [[PubMed](#)]
13. Xu, D.; Zhao, Y.; Sun, K.; Gao, B.; Wang, Z.; Jin, J.; Zhang, Z.; Wang, S.; Yan, Y.; Liu, X.; et al. Cadmium adsorption on plant-and manure-derived biochar and biochar-amended sandy soils: Impact of bulk and surface properties. *Chemosphere* **2014**, *111*, 320–326. [[CrossRef](#)] [[PubMed](#)]
14. Ye, X.; Kang, S.; Wang, H.; Li, H.; Zhang, Y.; Wang, G.; Zhao, H. Modified natural diatomite and its enhanced immobilization of lead copper and cadmium in simulated contaminated soils. *J. Hazard. Mater.* **2015**, *289*, 210–218. [[CrossRef](#)] [[PubMed](#)]
15. Li, H.; Dong, X.; Da Silva, E.B.; De Oliveira, L.M.; Chen, Y.; Ma, L.Q. Mechanisms of metal sorption by biochars: Biochar characteristics and modifications. *Chemosphere* **2017**, *178*, 466–478. [[CrossRef](#)] [[PubMed](#)]
16. Nguyen, B.T.; Lehmann, J.; Kinyangi, J.; Smernik, R.; Riha, S.J.; Engelhard, M.H. Long-term black carbon dynamics in cultivated soil. *Biogeochemistry* **2009**, *92*, 163–176. [[CrossRef](#)]
17. Meng, J.; Tao, M.; Wang, L.; Liu, X.; Xu, J. Changes in heavy metal bioavailability and speciation from a Pb-Zn mining soil amended with biochars from co-pyrolysis of rice straw and swine manure. *Sci. Total Environ.* **2018**, *633*, 300–307. [[CrossRef](#)]
18. Qi, F.; Lamb, D.; Naidu, R.; Bolan, N.S.; Yan, Y.; Ok, Y.S.; Rahman, M.M.; Choppala, G. Cadmium solubility and bioavailability in soils amended with acidic and neutral biochar. *Sci. Total Environ.* **2018**, *610–611*, 1457–1466. [[CrossRef](#)]
19. Grewal, A.; Abbey, L.; Gunupuru, L.R. Production, Prospects and Potential Application of Pyrolygneous Acid in Agriculture. *J. Anal. Appl. Pyrolysis* **2018**, *135*, 152–159. [[CrossRef](#)]
20. Jin, X.; Wu, X.; Zhang, H.; Jiang, X.; Huang, Z.; Liu, Y.; Fang, M.; Min, X. Novel humic acid-based carbon materials: Adsorption thermodynamics and kinetics for cadmium(II) ions. *Colloid Polym. Sci.* **2018**, *296*, 537–546. [[CrossRef](#)]
21. Pukalchik, M.; Mercl, F.; Terekhova, V.; Tlustoš, P. Biochar wood ash and humic substances mitigating trace elements stress in contaminated sandy loam soil: Evidence from an integrative approach. *Chemosphere* **2018**, *203*, 228–238. [[CrossRef](#)]
22. Zhang, Y.J.; Ou, J.L.; Duan, Z.K.; Xing, Z.; Wang, Y. Adsorption of Cr (VI) on bamboo bark-based activated carbon in the absence and presence of humic acid. *Colloids Surface A* **2015**, *481*, 108–116. [[CrossRef](#)]
23. Chen, D.; Liu, X.; Bian, R.; Cheng, K.; Zhang, X.; Zheng, J.; Joseph, S.; Crowley, D.; Pan, G.; Li, L. Effects of biochar on availability and plant uptake of heavy metals—A meta-analysis. *J. Environ. Manag.* **2018**, *222*, 76–85. [[CrossRef](#)] [[PubMed](#)]
24. Cang, L.; Zhou, D.M.; Wang, Q.Y.; Wu, D.Y. Effects of electrokinetic treatment of a heavy metal contaminated soil on soil enzyme activities. *J. Hazard. Mater.* **2009**, *172*, 1602–1607. [[CrossRef](#)]
25. Zhu, J.; Gao, W.; Ge, L.; Zhao, W.; Zhang, G.; Niu, Y. Immobilization properties and adsorption mechanism of nickel (II) in soil by biochar combined with humic acid-wood vinegar. *Ecotoxicol. Environ. Saf.* **2021**, *215*, 112159. [[CrossRef](#)] [[PubMed](#)]
26. Kulikowska, D.; Gusiatin, Z.M.; Bułkowska, K.; Klik, B. Feasibility of using humic substances from compost to remove heavy metals (Cd Cu Ni Pb Zn) from contaminated soil aged for different periods of time. *J. Hazard. Mater.* **2015**, *300*, 882–891. [[CrossRef](#)]
27. Santos, N.M.D.; Accioly, A.M.D.A.; Nascimento, C.W.A.D.; Silva, I.R.; Santos, J.A.G. Bioavailability of lead using chemical extractants in soil treated with humic acids and activated carbon. *Rev. Ciênc. Agrônômica* **2015**, *46*, 663–668. [[CrossRef](#)]
28. Zhu, J.; Gao, W.; Zhao, W.; Ge, L.; Zhu, T.; Zhang, G.; Niu, Y. Wood vinegar enhances humic acid-based remediation material to solidify Pb (II) for metal-contaminated soil. *Environ. Sci. Pollut. Res.* **2020**, *28*, 12648–12658. [[CrossRef](#)]
29. Dong, Y.; Lin, H.; Zhao, Y.; Menzembere, E.R.G.Y. Remediation of vanadium-contaminated soils by the combination of natural clay mineral and humic acid. *J. Clean. Prod.* **2021**, *279*, 123874. [[CrossRef](#)]
30. Sungur, A.; Soylak, M.; Ozcan, H. Investigation of heavy metal mobility and availability by the BCR sequential extraction procedure: Relationship between soil properties and heavy metals availability. *Chem. Spec. Bioavailab.* **2014**, *26*, 219–230. [[CrossRef](#)]
31. Chen, H.; Li, Q.; Wang, M.; Ji, D.; Tan, W. XPS and two-dimensional FTIR correlation analysis on the binding characteristics of humic acid onto kaolinite surface. *Sci. Total Environ.* **2020**, *724*, 138154. [[CrossRef](#)]
32. Vieira, R.S.; Oliveira, M.L.M.; Guibal, E.; Rodríguez-Castellón, E.; Beppu, M.M. Copper mercury and chromium adsorption on natural and crosslinked chitosan films: An XPS investigation of mechanism. *Colloids Surface A* **2011**, *374*, 108–114. [[CrossRef](#)]

33. Rong, Q.; Zhong, K.; Huang, H.; Li, C.; Zhang, C.; Nong, X. Humic acid reduces the available cadmium copper lead and zinc in soil and their uptake by tobacco. *Appl. Sci.* **2020**, *10*, 1077. [[CrossRef](#)]
34. Wang, Z.; Mi, Z.; Zheng, C.; Li, W.; Wang, W.; Wang, H. Effect of biochar on the bioavailability and transformation of heavy metals in soil of mining area. *Chem. Ind. Eng. Prog.* **2019**, *38*, 2977–2985. (In Chinese)
35. Gu, P.; Zhang, Y.; Xie, H.; Wei, J.; Zhang, X.; Huang, X.; Wang, J.; Lou, X. Effect of cornstalk biochar on phytoremediation of Cd-contaminated soil by *Beta vulgaris* var *cicla* L. *Ecotoxicol. Environ. Saf.* **2020**, *205*, 111144. [[CrossRef](#)]
36. Tawfik, A.S. Isotherm kinetic and thermodynamic studies on Hg (II) adsorption from aqueous solution by silica-multiwall carbon nanotubes. *Environ. Sci. Pollut.* **2015**, *22*, 16721–16731. [[CrossRef](#)]
37. Meissl, K.; Smidt, E.; Schwanninger, M. Prediction of humic acid content and respiration activity of biogenic waste by means of Fourier transform infrared (FTIR) spectra and partial least squares regression (PLS-R) models. *Talanta* **2007**, *72*, 791–799. [[CrossRef](#)]
38. Chowdhury, I.H.; Ghosh, S.; Basak, S.; Naskar, M.K. Mesoporous CuO-TiO₂ microspheres for efficient catalytic oxidation of CO and photodegradation of methylene blue. *J. Phys. Chem. Solids* **2017**, *104*, 103–110. [[CrossRef](#)]
39. Schrader, I.; Wittig, L.; Richter, K.; Vieker, H.; Beyer, A.; Golzhauser, A.; Hartwig, A.; Swiderek, P. Formation and structure of copper (II) oxalate layers on carboxy-terminated self-assembled monolayers. *Langmuir* **2014**, *30*, 11945–11954. [[CrossRef](#)] [[PubMed](#)]
40. Rodríguez, F.J.; Schlenger, P.; García-Valverde, M. Monitoring changes in the structure and properties of humic substances following ozonation using UV–Vis FTIR and ¹H NMR techniques. *Sci. Total Environ.* **2016**, *541*, 623–637. [[CrossRef](#)]
41. Bai, H.; Luo, M.; Wei, S.; Jiang, Z.; He, M. The vital function of humic acid with different molecular weight in controlling Cd and Pb bioavailability and toxicity to earthworm (*Eisenia fetida*) in soil. *Environ. Pollut.* **2020**, *261*, 114222. [[CrossRef](#)]
42. Liu, Y.; Wang, T.; Qu, G.; Jia, H. High-efficient decomplexation of Cu-HA by discharge plasma: Process and mechanisms. *Sep. Purif. Technol.* **2020**, *248*, 117137. [[CrossRef](#)]
43. Hiyasmin, R.L.B.; Sang, C.L. Pyroligneous acids enhance phytoremediation of heavy metal-contaminated soils using mustard. *Commun. Soil Sci. Plan* **2017**, *48*, 2061–2073. [[CrossRef](#)]

Disclaimer/Publisher’s Note: The statements, opinions and data contained in all publications are solely those of the individual author(s) and contributor(s) and not of MDPI and/or the editor(s). MDPI and/or the editor(s) disclaim responsibility for any injury to people or property resulting from any ideas, methods, instructions or products referred to in the content.